CLINICAL ORAL IMPLANTS RESEARCH

Jean-Pierre Carrel
Anselm Wiskott
Mira Moussa
Philippe Rieder
Susanne Scherrer
Stéphane Durual

A 3D printed TCP/HA structure as a new osteoconductive scaffold for vertical bone augmentation

Authors' affiliations:
Jean-Pierre Carrel, Department of maxillofacial and oral surgery, Division of oral and maxillofacial pathology (HUG), School of dental medicine, Geneva, Switzerland
Anselm Wiskott, Mira Moussa, Philippe Rieder, Susanne Scherrer, Stéphane Durual, Division of fixed prosthodontics and biomaterials, School of Dental medicine, University of Geneva, Geneva, Switzerland

Corresponding author:
Dr. Stéphane Durual
Division of fixed prosthodontics and biomaterials
School of Dentistry, University of Geneva
19, rue Barthélemy-Menn
1205 Geneva, Switzerland
Tel.: +41 22 379 40 92
Fax: +41 22 379 41 14
e-mail: stephane.durual@unige.ch

No benefit of any kind has been or will be received either directly or indirectly by the authors.

Date:
Accepted 28 September 2014

To cite this article:
Carrel J-P, Wiskott A, Moussa M, Rieder P, Scherrer S, Durual S. A 3D printed TCP/HA structure as a new osteoconductive scaffold for vertical bone augmentation. *Clin. Oral Impl. Res.* **00**, 2014,1–8.
doi: 10.1111/clr.12503

Key words: animal experiments, bone regeneration, bone substitutes, guided tissue regeneration

Abstract

Introduction: OsteoFlux® (OF) is a 3D printed porous block of layered strands of tricalcium phosphate (TCP) and hydroxyapatite. Its porosity and interconnectivity are defined, and it can be readily shaped to conform the bone bed's morphology. We investigated the performance of OF as a scaffold to promote the vertical growth of cortical bone in a sheep calvarial model.

Materials and methods: Six titanium hemispheres were filled with OF, Bio-Oss (particulate bovine bone, BO), or Ceros (particulate TCP, CO) and placed onto the calvaria of 12 adult sheep (6 hemispheres/sheep). Histomorphometric analyses were performed after 8 and 16 weeks.

Results: OF led to substantial vertical bone growth by 8 weeks and outperformed BO and CO by a factor 2 yielding OF 22% ± 2.1; BO 11.5% ± 1.9; and CO 12.9% ± 2.1 total new bone. 3 mm away from the bony bed, OF led to a fourfold increase in new bone relative to BO and CO ($n = 8$, $P < 0.002$). At 16 weeks, OF, BO, and CO behaved similarly and showed marked new bone synthesis. A moderate degradation was observed at 16 weeks for all bone substitutes.

Conclusion: When compared to existing bone substitutes, OF enhances vertical bone growth during the first 2 months after implantation in a sheep calvarial model. The controlled porous structure translated in a high osteoconductivity and resulted in a bone mass 3 mm above the bony bed that was four times greater than that obtained with standard substitutes. These results are promising but must be confirmed in clinical tests.

Bone regeneration is of importance in a number of surgical disciplines such as neurosurgery, orthopedics, and traumatology. In dental surgery, it also applies to the reconstruction of defects of the jaw bones. Indeed, after a traumatic episode, regenerative processes do not take place spontaneously and are often insufficient in terms of resulting tissue volume. A scaffold of natural or synthetic origin must be used to initiate and drive bone growth by steering the kinetics of wound healing. Therefore, an ideal bone graft or bone substitute should provide a template for osteoconduction, growth factors for osteopromotion, and scaffolding for internal osteogenesis (Draenert et al. 2014). The resulting newly formed bone will then seamlessly integrate with the bony bed.

Autogenous grafts (i.e., pieces of live bone taken from another site in the patient) are considered ideal as they contain (i) osteoprogenitor cells and osteoblasts capable of producing new bone, (ii) a structural matrix that acts as a scaffold, and (iii) bioactivators of bone formation. Still, the amount of autogenous bone that can be extracted from a given patient is often limited, and the donor sites' morbidity may reach 25% (Myeroff & Archdeacon 2011). The alternatives to autologous bone are allografts (i.e., bone harvested from human cadavers), xenografts (bone obtained from a different animal species), and artificial materials (Esposito et al. 2009). Xenografts and artificial materials are mostly used. Ultrastructurally, the material should be porous whereby the pores must be interconnected to permit the influx of mesenchymal cells, osteoblasts, and the development of a vascular supply (Karageorgiou & Kaplan 2005). The typical xenograft is produced by removing the organic phase from pieces of bovine bone—a procedure which consists in chemically extracting all organic compounds at a temperature of 300°C. This virtually eliminates the antigenic potential but preserves the mineral phase structure and

composition. The substitute thus presents a standard trabecular architecture and will act as a natural osseoconductor (possibly osseoinductor) (Gross 1997; Richardson et al. 1999). However, its animal origin limits patient acceptance due to infection hazard by prion diseases (Wenz et al. 2001). Intrinsically, synthetic bone substitutes do not carry these risks. Chemically, they are combinations of calcium, phosphates, carbonates, sulfates, and silicon oxides. Potassium, sodium, and manganese are also found (Polo-Corrales et al. 2014). A most prominent representative in this category is biphasic calcium phosphate—a combination of hydroxyapatite (HA) and tricalcium phosphate (TCP) formulated as an optimum balance between the most stable form of HA and most soluble form of TCP (Daculsi 1998).

Typically, bone substitutes of natural or synthetic origin are used in granular form. The granules are packed onto the bone crest and covered with a resorbable membrane that ensures primary stability and prevents leakage of the particles. Alternatively, the materials are also available as blocks, but these never became popular for various reasons, the main being a lack of "shapeability" and the blocks being perceived as fragile (Simion et al. 2006; Felice et al. 2009). In this regard, 3D printing is an attractive option as it may overcome the above limitations. Its major advantages are as follows: (i) The materials used are purely synthetic, (ii) a regular arrangement of interconnected pores that is controllable in size and patency can be constructed, (iii) the geometry of the constructs can be adapted to the recipient bone bed as well as to the intended bone volume, and (iv) the constructs provide support to the overlying soft tissue.

Such a three-dimensional structure has recently been developed. Hence, the objective of this study was to evaluate its performance both histologically and histomorphometrically in a model of guided bone regeneration in sheep.

Material and methods

Experimental design

The experiment was conducted on 12 sheep. Six locations were available on each skull (occipital left and right, median left and right, frontal left and right). After initial acclimation, six randomly allotted titanium hemispheres filled either with (i) 3D printed constructs, (ii) particulate material of bovine origin, (iii) synthetic particles, or (iv) plain blood coagulum (negative control) were placed on the calvarium of each animal (Table 1). Randomization was obtained by drawing lots with the following constraints. (i) Each sheep had to receive at least one of the three substitutes but (ii) no sheep could be fitted with more than two samples of the same substitute. (iii) Each of the three substitutes was to be placed at least once in one of the six positions. (iv) The four controls (no substitute) had to be placed on different animals and (v) distributed over the occipital, the median, and the frontal sites. Six animals were sacrificed after 8 weeks and six after 16 weeks. The skulls were block-sectioned and subjected to histomorphometric analysis. Outcomes were analyzed in terms of the relative volumes of bone substitute and new bone tissue.

Bone substitutes

The following bone substitute materials were subjected to analysis.

1. The 3D printed block (OsteoFlux®; Vivos-Dental, Villaz-St-Pierre, CH). These blocks are made of orthogonally layered cylindrical filaments, 400 μm in diameter separated by spaces 250 μm in width. Upon printing, the filaments are deposited as a high-viscosity paste which then sets to a hard consistency. They are made of synthetic calcium phosphate with a calcium-to-phosphate ratio of 1.43 (range 1.35–1.5). The main phases are calcium phosphates in the form of α-TCP and microcrystalline, calcium-deficient HA. The construct's macroporosity ranges between 40 and 50% and the total porosity between 50 and 65% (Fig. 1a,b).
2. A particulate substitute of bovine origin (Bio-Oss®, Geistich Pharma, Wolhusen, CH). This material is made of granules, 0.25–1 mm in diameter. It is resorbable and presents a natural bone microarchitecture with a total porosity of 60%.
3. A synthetic particulate substitute (Ceros®, Thommen Medical, Grenchen, CH). This product presents itself as granules 0.5–0.7 mm in diameter. It is made of pure β-TCP and hence resorbable. The granules have a total porosity of 60%.

For the sake of simplicity, OsteoFlux®, Bio-Oss®, and Ceros® will be referred to as OF, BO, and CO hereafter.

Hemispheres and placement of bone substitutes

The hemispheres were machined out of titanium (cpTi-gr2) with an inner diameter of 10 mm, an outer diameter of 11 mm, and a height of 5 mm. OF blocks were printed to a perfect fit inside the hemispheres (Fig. 2a) and were gamma sterilized before use.

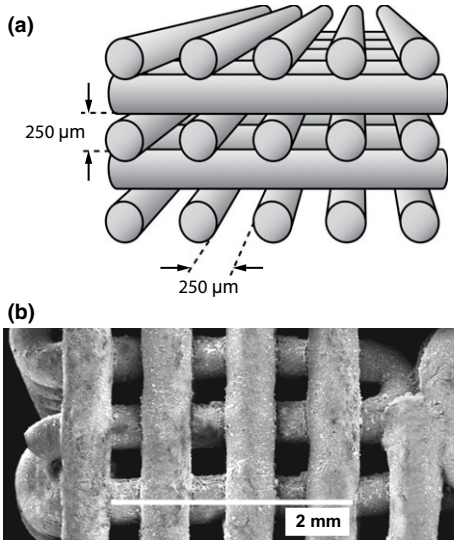

Fig. 1. (a). Schematic drawing of the 3D block's (OsteoFlux®) microstructure with a regular arrangement of interconnected pores. (b). SEM view.

At the time of surgery, the OF blocks were loaded with autologous blood and then placed into the hemispheres. BO and CO were prepared to a homogeneous blood granules paste and then gently packed into the cups to ensure optimal density. The control spheres were merely filled with blood. The hemispheres were placed onto the skull immediately after being filled.

Animals

Twelve adult BMC sheep (female, 2.5–4 years, 69–87 kg) were included in the study (Eymin Breeding, Seyssuel, F). The animals underwent an acclimation period of one week prior to surgery. The experiment was conducted in a dedicated facility [NAMSA, Chasse sur Rhône, FR (ISO/CEI 17025)]. In line with European requirements (European Directive 2010/63/EU), all animal experiments were approved by the local veterinary committee (NAMSA Ethical Committee, French Ministry of Agriculture).

Surgical procedure

The animals underwent general anesthesia. They were deprived of food (24 h) and water (12 h) prior to surgery to prevent vomiting. A prophylactic antibiotic coverage was dispensed 1 day before and up to 2 weeks after the surgery [amoxicillin-Duphamox, Pfizer, Fort Dodge, IA, USA, i.m. every 2 days (15 mg/kg) and enrofloxacin-Baytril 5%, Bayer Pharma, Leverkusen, DE s.c. daily (5 mg/kg)]. The animals first received an analgesic treatment (flunixine-Meflosyl i.m.

Pfizer (2 mg/kg), and buprenorphine-Buprecare s.c. (0.01 mg/kg), Animal care, York, UK). Anesthesia was induced by an intravenous injection of a mixture of thiopental–Nesdonal (750 mg, Merial, Lyon, FR)—pentobarbital sodium (273 mg, CEVA, Libourne, FR)—atropine sulfate (1 mg, Aguettant, Lyon, FR) before intubation. Deep anesthesia was obtained using 2% isoflurane–Aerrane (Baxter, Deerfield, IL, USA) in pure oxygen. A rectal temperature probe and a rumen tube were placed. Heart function, temperature, and oxygen saturation were monitored. Iso-volumetric conditions were maintained by infusion of a ringer lactate solution during the entire procedure. The surgical areas were shaved, and the skin was scrubbed with povidone iodine (Vetoquinol, Lure, FR), wiped with isopropyl alcohol, painted with povidone iodine, and draped.

A midline incision was made through the skin, from the orbits to the external occipital protuberance. The temporalis muscles were elevated subperiosteally from the frontal and parietal bone and bilaterally retracted. On each side of the median suture, three circumferential grooves, 10 mm in diameter and approximately 0.5 mm in depth, were trephined under saline irrigation. In each of the resulting circles, 11 intramedullary holes (1 mm in diameter, ca. 2 mm in depth) were drilled with a round bur to allow bone cell migration from the marrow to the surface. Thus, in each animal, six grafting sites made of a cortical bone plate penetrated by 11 transcortical perforations were produced (Fig 2b). Primary stability of the hemispheres was ensured by the clipping effect of the titanium hemisphere onto the bone (Fig. 2c). Each animal received at least one of each bone substitutes. The distribution of the bone substitutes within the six positions was determined from a table of random allocations (SPSS). Wound closure was carried out in three planes. The deeper tissues were closed using a discontinuous resorbable suture (Vicryl 3-0, Ethicon, Sommerville, NJ, USA). A povidone iodine solution was applied before closing the subcutaneous tissues with the resorbable suture material. The skin was closed with a continuous non-resorbable suture (Prolene 3-0, Ethicon) and disinfected with a spray of oxytetracycline (Oxytetrin, Merck-MSD, White house station, NJ, USA).

Postoperative pain was minimized by subcutaneous injections of buprenorphine (Buprecare, Animalcare, UK) 0.01 mg/kg, twice daily for 2 days. Inflammation was controlled for 7 days by daily intramuscular injections of flunixin (Meflosyl, Zoetis, Florham Park, NJ, USA) 2 mg/kg. The wounds were disinfected until 2 days past sutures removal which itself was carried out after complete healing.

The animals were euthanized 8 and 16 weeks after placement of the hemi-

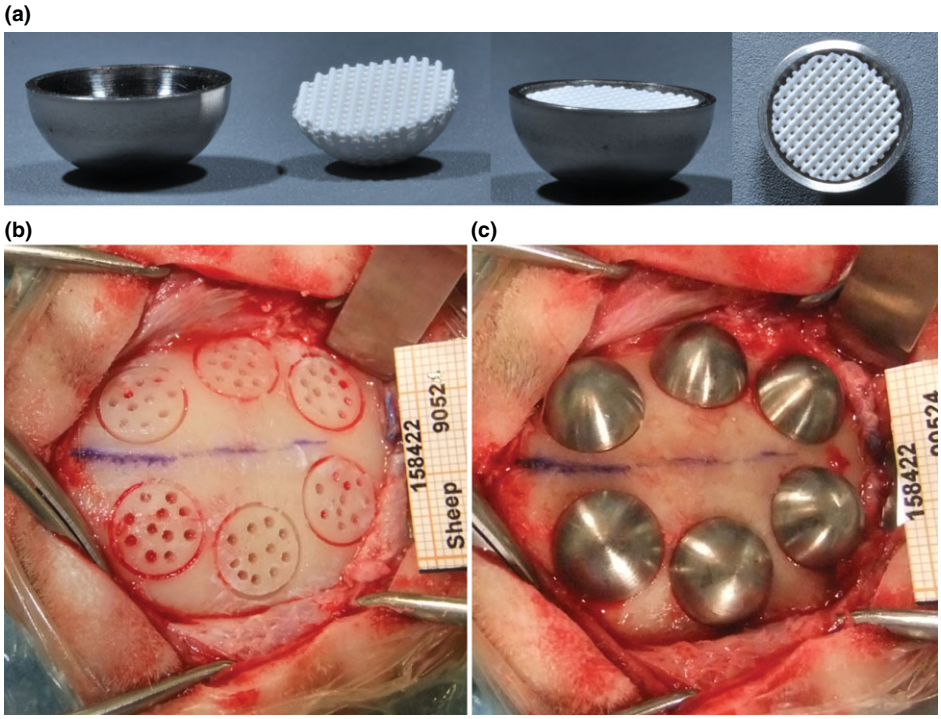

Fig. 2. (a). Titanium hemispheres filled with OsteoFlux®. (b). Circular grooves with transcortical perforations prior to fixation of the titanium hemispheres filled with bone substitute material (c).

Table 1. **Specimens analyzed**

Healing period	Bone substitute	Number of specimen analyzed (*n*)
8 weeks	Coagulated blood (control)	4
	3D printed construct	8
	Bovine particulate substitute	8
	Synthetic particulate substitute	8
16 weeks	Coagulated blood (control)	4
	3D printed construct	8
	Bovine particulate substitute	8
	Synthetic particulate substitute	8
	Total placed: 56	Total analyzed: 56

Table 2. **Histopathologic scoring system (semiquantitative)**

	Score				
Cell type/Response	0	1	2	3	4
Polymorphonuclear cells (PMN)	0	Rare, 1–5/phf	5–10/phf	Heavy infiltrate	Dense
Lymphocytes (Lc)	0	Rare, 1–5/phf	5–10/phf	Heavy infiltrate	Dense
Plasma cells (Plc)	0	Rare, 1–5/phf	5–10/phf	Heavy infiltrate	Dense
Macrophages (Ma)	0	Rare, 1–5/phf	5–10/phf	Heavy infiltrate	Dense
Giant cells/osteoclastic cells (Gc/Oc)	0	Rare, 1–2/phf	3–5/phf	Heavy infiltrate	Sheets
Osteoblasts (Ob)	0	Slight, equivalent to normal bone	Moderate, > normal bone	Marked, >> normal bone	Highly marked

phf, per high-powered (400×) field.

spheres. Immediately after sacrifice, the skulls were dissected and immersed in neutral buffer and 10% formalin.

Histological preparation, histopathologic, and histomorphometric analysis

After complete fixation, the skull was block-sectioned to isolate each hemisphere. The blocks were (i) rinsed for 3 h with tap water, (ii) dehydrated in alcohol solutions of increasing concentration, (iii) cleared in xylene, and (iv) embedded in polymethyl methacrylate resin (Merck-MSD, White house station, NJ, USA). Using a precision band saw (EXAKT, Oklahoma city, OK, USA), undecalcified specimens were obtained by sectioning the titanium caps perpendicular to the bone surface midway through the hemispheres. Then, the specimens were thinned out to a thickness of 30–40 μm by microgrinding and polished (Mecapol P320, Presi, Grenoble, FR). Finally, they were stained with modified paragon. The sections were digitized with a light microscope (Eclipse 80i, Nikon, Tokyo, JP) coupled with a digitizing camera (Allied Vision Technologies, Taschenweg, DE). Single pictures of high-power fields at 10× magnification were assembled to generate large overview images.

Bone substitute and new bone tissue were scribed using a software for image analysis (Calopix viewer, Tribvn, Chatillon, FR). The structures of interest were delimited manually using a graphical pad on the entire surface inside the titanium hemispheres, that is, from the external cortical limit of the bony bed to the internal limit of the hemispheres. The amount of new bone and bone substitute was expressed as percentages of the total volume under the hemispheres. Artifacts and/or broken tissues were excluded from the computations. The histopathologic evaluation was performed using the scoring system described in Table 2 (ISO 10993-6 standard).

Statistical analysis

The histomorphometrical data were checked for normal distribution and equivalence of variances. Unpaired *t*-tests were used to compare OF ($n = 8$) to BO ($n = 8$) or CO ($n = 8$) at 2 or 4 months. For the analyses on horizontal segmentation, only groups within a slice were compared. Owing to the multiple comparisons performed, Bonferroni's correction was applied and the null hypothesis rejected at $P < 0.025$.

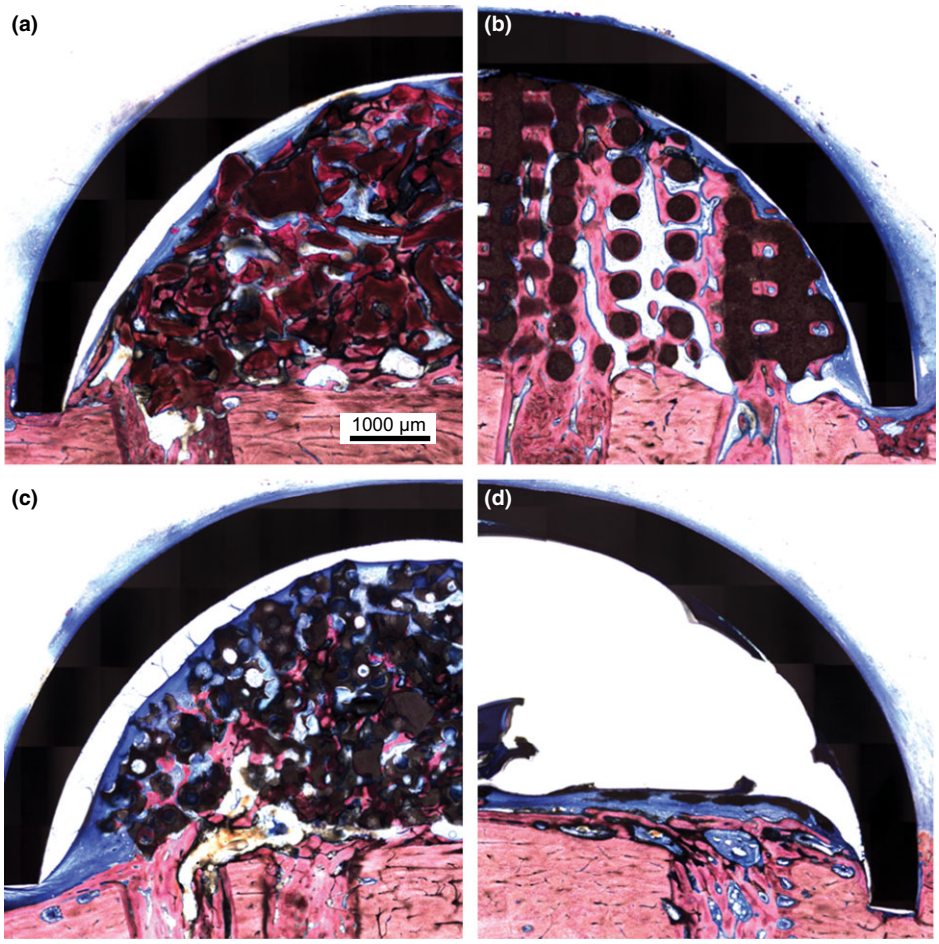

Fig. 3. Hemi-slide showing the bone substitutes' engraftment under the titanium hemispheres at 8 weeks. (a) BO appears as dark red particles surrounded and bridged by new bone (light pink), mainly in the vicinity of the bony bed (salmon pink). Note that the transcortical perforation is filled with new bone. (b) OF appears as brown circles or rounded polygons depending on the angle of cutting. The newly formed bone sprouts from the transcortical perforations and then develops into vertical columns from the bony bed up to the titanium hemispheres. The bone is often lined by unmineralized bone (blue). Note that the horizontal (i.e., perpendicular) canals are filled with new bone even at the top of the construct and include a central vessel system. (c) CO appears as gray particles surrounded and bridged by new bone, mainly in the vicinity of the bony bed. Note that CO's macropores are occasionally filled with new bone. (d) The control site shows a complete healing of the transcortical perforation with some new bone covering the old bony bed. Note the remnant of coagulated blood (purple). (BO: Bio-Oss®, CO: Ceros®, OF: OsteoFlux®).

Table 3. **Semiquantitative histopathologic evaluation (scoring Table 2, $n = 8$, mean ± SD)**

Time	Bone substitute $n = 8$	Polymorphonuclear cells	Lymphocytes	Plasma cells	Macrophages	Giant cells/Osteoclastic cells	Osteoblastic cells
8 weeks	OsteoFlux	0	0	0	1.1 ± 0.3	0.9 ± 0.3	2.6 ± 0.5
	Bio-Oss	0	0	0	1	1	1.3 ± 0.7
	Ceros	0	0	0	1.4 ± 0.5	0.8 ± 0.4	1.6 ± 0.5
16 weeks	OsteoFlux	0	0	0	1.3 ± 0.4	1	2 ± 0.5
	Bio-Oss	0	0	0	0.8 ± 0.7	1.1 ± 0.3	1.6 ± 0.5
	Ceros	0	0	0	2 ± 0.5	2 ± 0.5	1.8 ± 0.7

Results

Macroscopically, at necroscopy, none of the 56 sites presented signs of inflammation. All hemispheres remained as placed both at 8 and 16 weeks.

Histopathologic evaluation

Prior to histomorphometric analysis, a histopathologic evaluation of inflammatory and bone cells was performed. The scoring system and the results are presented in Tables 2 and 3. No inflammatory cell infiltrate was detected on any site. Macrophages, giant cells, and osteoclasts, that is, the cells in charge of the degradation of the bone substitute and bone remodeling, were rarely seen at 8 and 16 weeks. A higher number, however, were noted next to the synthetic particles (CO) at 16 weeks. At 8 weeks, the density of bone cells exceeded that of normal bone on all substitutes whereby the 3D printed blocks contained twice as many osteoblasts as the particulate substitutes (BO and CO). At 16 weeks, the density of osteoblasts was moderately increased and equal among the 3 materials.

Histologic evaluation

At 8 weeks, the hemispheres were covered by a fibrous layer. The circular grooves that stabilized the hemispheres were often filled with new bone (Fig. 3a,b) which somewhat lifted the cups out of their bone bed. As a consequence, on the inside of the cups, a layer of connective tissue developed between the metal and the substitute materials (Fig. 3a–c). In the control sites (Fig. 3d), the hemispheres were almost empty although some minor bone growth was noted.

OF samples showed evident signs of osteoconduction along the vertical canals of the construct which often extended to the top of the structure. The newly formed bone clearly sprouted from the intramedullary perforations. The horizontal canals were also largely filled with new bone, and a central vasculature had developed (Figs 3b and 4e,f). OF integrated well, as shown by the intimate contact between the newly formed bone and the material (Fig. 4b–f). The bone was characterized by marked osteoblastic activity (Figs 3b and 4a–f), even at large distances from the calvarial plate (Fig. 4b,c). A sight evidence of material degradation was observed, mainly at the base of the block (Fig. 4d). The remaining space was filled with connective and highly vascularized osteoid tissue (Figs 3b and 4b,c,f).

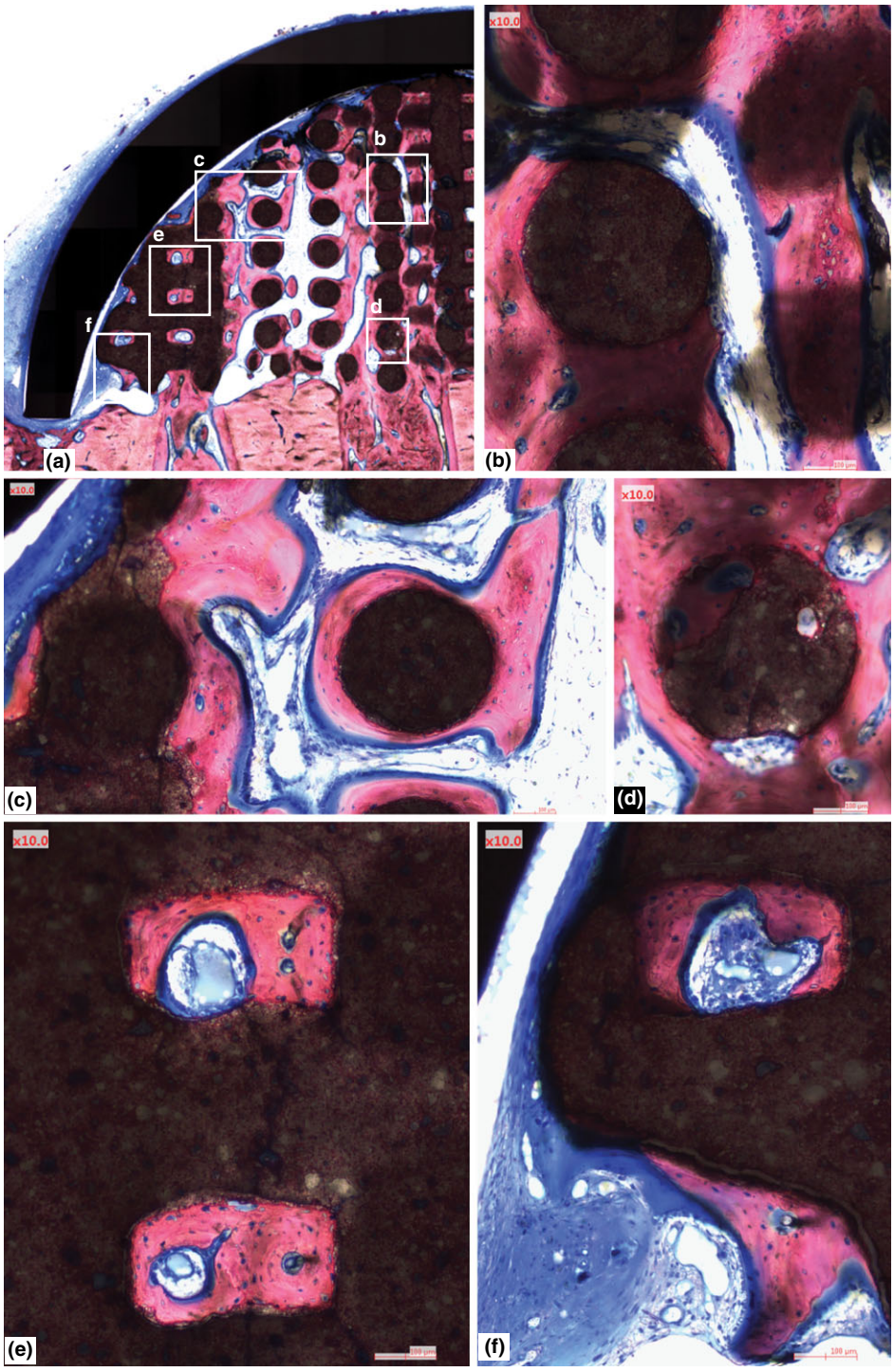

Fig. 4. Higher magnifications of a hemi-slide (a) showing various zones within the OF scaffold at 8 weeks. At a larger distance from the bone bed (b,c), the material integrates well. There is an intimate contact between bone and substitute material. A marked osteogenesis is evident as shown by the rows of osteoblasts lining the new bone. The horizontal canals (i.e., perpendicular) are largely filled with new bone and a central vasculature (e, f). A highly vascularized osteoid tissue fills the remaining space (f). A slight resorption of the material is observable at the basis of the construct (d), with a notable amount of osteoclasts. (OF: OsteoFlux®)

BO and CO samples behaved very much alike, both showing slight signs of vertical osseoconduction (Fig. 3a,c). The newly formed bone was heterogeneously distributed. The bone surrounded the particles mainly along the base of the material but without noticeable continuity with the bony bed or the intramedullary perforations. The particles integrated well and the bone demonstrated a moderate osteoblastic activity.

There was no evidence of material degradation at this stage. The space between the particles was filled by connective and highly vascularized osteoid tissue.

At 16 weeks, all three materials presented similar outcomes regarding osseoconduction and osseointegration. The spaces were almost entirely filled with new bone (80–90%). In OF, a slight differentiation into adipocytic bone marrow was occasionally observed in some bone lacunae. CO particles showed evident signs of degradation as compared to OF and BO.

Histomorphometric evaluation

The histomorphometric analyses addressed the bone substitute and the new bone tissue that had formed under the hemispheres.

At 8 weeks, the new bone volume (NBV) in OF exceeded that of BO and CO by 1.8 times. NBV under the hemispheres reached 23 ± 1.6% in OF as compared to 13.6 ± 1.5% and 13.8 ± 1.5% in BO and CO, respectively (Fig. 5a). More specifically, in the first 2 mm above the bony bed, there were no significant differences between the 3 substitutes. For all three, NBV reached ca. 30% of the volume between 0 and 1 mm and ca. 20% of the volume between 1 and 2 mm (Fig. 6a). However, in the 2–3 mm range, NBV in OF samples exceeded that in BO and CO by approx. 2 times (OF: 19 ± 3%, BO: 9.9 ± 2%, CO: 8.4 ± 2%) and above 3 mm by 3–5 times (OF: 18 ± 3%, BO: 5 ± 1%, CO: 3 ± 1%) (Fig. 6a).

For all three materials, there was about 25% of NBV deposited in the 1–2 mm range. In the 2–3 mm range, NBV amounted to 18 ± 2% in OF, 11 ± 3% in CO, and 13 ± 3% in BO. Beyond 3 mm, NBV amounted to 10 ± 1% in OF, 2 ± 1% in CO, and 4 ± 1% in BO (Fig. 6c). The large majority of the bone was deposited in close contact with the bony bed (i.e., 0–1 mm range) with amounts of approx. 60% in BO and CO vs. 45% in OF.

At 16 weeks, there was a tendency toward a reversal, the total NBV reaching 35 ± 2%, 39 ± 2%, and 43 ± 6% in OF, BO, and CO, respectively (Fig. 5a). The vertical distribution of the new bone was equivalent in all bone substitutes, that is, about 10% above 3 mm, about 20% between 2 and 3 mm, about 30% between 1 and 2 mm, and about 40% between 0 and 1% (Fig. 6a,c).

Regarding the volume of the bone substitute (BSV) under the hemispheres, there were no differences from 8 to 16 weeks in OF and BO with amounts at about 45% and 40%, respectively. In contrast, BSV decreased from 33% to 19% in CO (Fig. 5b).

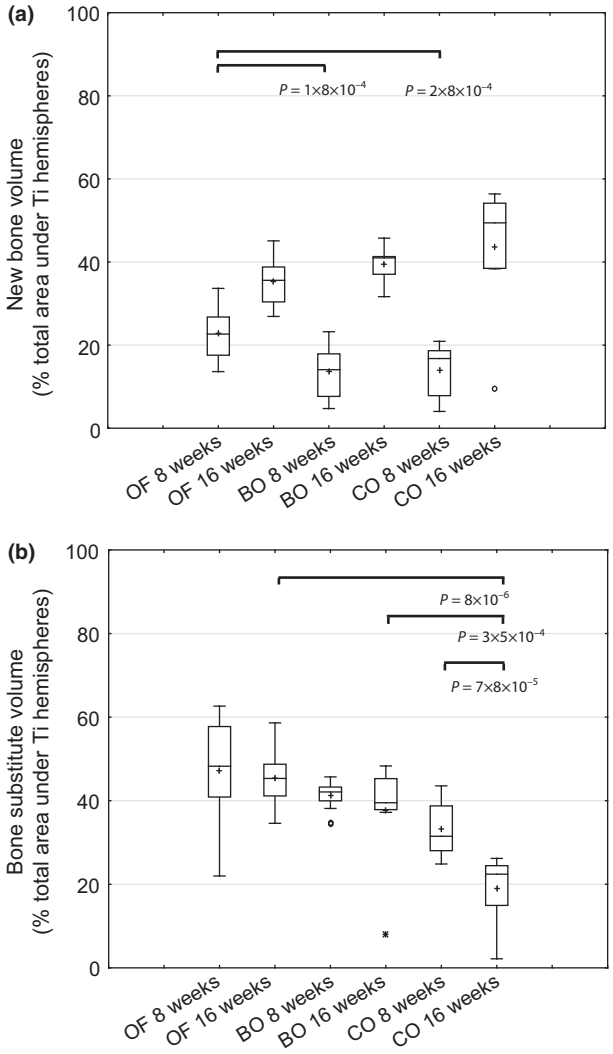

Fig. 5. Histomorphometrical assessment of new bone volume (a) and volume of bone substitute (b) under the hemispheres at 8 and 16 weeks (n = 8 for each column). Brackets and P values indicate significant differences. Horizontal line: median. Boxes: 25-75%.+: mean. Bars: range of non-outliers. ○: outliers. ✱: extreme. (BO: Bio-Oss®, CO: Ceros®, OF: OsteoFlux®)

Discussion

The present work aimed at evaluating the performance of a 3D printed block of bone substitute (OsteoFlux®) in terms of osseoconduction and vertical bone regeneration in a calvarial sheep model. The deposition of new bone on the calvarium was analyzed 2 and 4 months after implantation and compared to two standard bone substitutes, that is, particulate materials of bovine origin (Bio-Oss®) and a synthetic β-TCP (Ceros®).

The calvarial model of a one wall defect in which the bone substitutes are maintained and protected by titanium cups was first used in rabbits (Yamada et al. 2003, 2008) and proved satisfactory. However, due to the small size of rabbit skulls, only two cups per animal could be placed. To overcome the problem, the same model was implemented on the calvaria of pigs (Busenlechner et al. 2008), thus permitting the simultaneous placement of 8 cups and the comparison of 4 bone substitutes. In their work, the authors placed small perforations into the cortex which permitted a migration of bone precursor cells from the bone marrow to the bone substitutes. The authors also established a size for the titanium cups in which the bone growth without substitute was minimal. One advantage of this model is the maximal preservation of the original bone bed as compared to models in which bone defects are artificially created. The cup model in essence reflects the typical clinical situation in dental surgery in which clinicians need more bone and want to preserve existent bone prior to reconstruction. The model thus truly tests the osseoconductive properties of the implanted material.

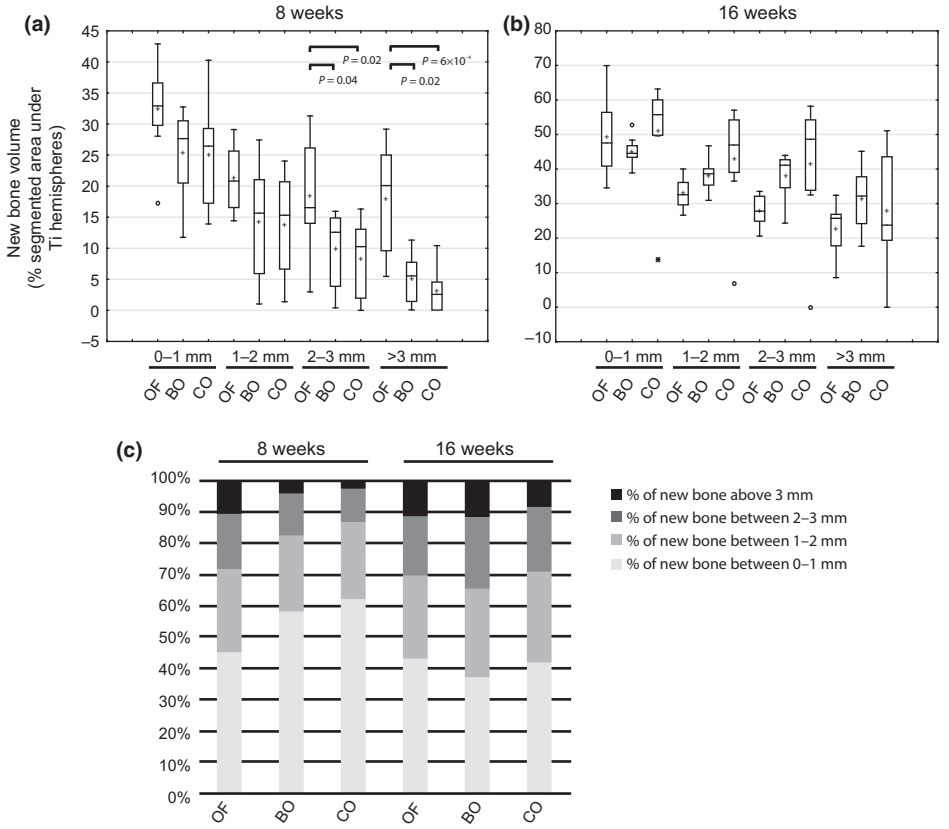

Fig. 6. New bone volume under the hemispheres segmented in 4 horizontal planes of 1 mm in height at 8 weeks (a) and 16 weeks (b). The proportion of new bone within the different planes is also summarized in a graphic (c). (n = 8 for each column). Brackets and P values indicate significant differences. Horizontal line: median. Boxes: 25-75%.+: mean. Bars: ⊹ range of non-outliers. ◯: outliers. ✱: extreme. (BO: Bio-Oss®, CO: Ceros®, OF: OsteoFlux®).

Sheep calvaria have been largely used for cranioplasty, distraction, and reconstruction studies with or without bone substitutes (Gosain et al. 2004; Kuemmerle et al. 2005; Eufinger et al. 2007)—the typical model being that of a critical size defect. The bone metabolism in sheep is similar to pigs and, as such, largely comparable to humans (Pearce et al. 2007). Therefore, in the present work, Yamada et al.'s model (Yamada et al. 2003, 2008) was implemented on sheep skulls [the dimensions of the cups were those of Busenlechner et al. (Busenlechner et al. 2008)].

Ultrastructurally, bone-inductive materials should be porous, and the pores must be interconnected to permit the influx of osteogenic cells. In this work, BO and CO were used as reference standards. BO is a bone substitute produced by removal of the organic phase from bovine bone and thus presents the trabecular architecture of natural osseous tissue. CO is a particulate resorbable bone substitute of synthetic origin made of pure beta-tricalcium phosphate (β-TCP). Both present an optimal total porosity of 60%, which is similar to that of natural bone.

Two differences, though, are readily apparent between the particulate materials and the 3D block. First, particles do not maintain volume well. If bone volume needs to be locally augmented, a stable scaffold will, by design, permit augmentations in the horizontal, as well as in the vertical direction (in dental surgery, the typical use of granulate substitutes is in the horizontal direction only). Second, in particulate materials, the arrangement of channels and pores is haphazard. We hypothesized that such an unorganized disposition may limit osseoconduction. One of the advantages of the 3D blocks is their linear pore structure which is controllable in size and patency over the entire length of the block. Such straight would thus favor the progression of a "mineralization front" with its accompanying vascular system. The total porosity of the constructs lies in the 60% range. The channels' diameter was set to 250 μm, a value that is in the middle of the pore sizes recommended for optimal osseoconduction (150–500 μm) (Hollister et al. 2005; Seitz et al. 2005).

During the first 2 months, after implantation, vertical bone growth around OF was significantly increased. The block's osteoconductivity translated in an amount of bone at 3 mm that was four times higher than that obtained with the other bone substitutes. The newly forming bone was guided from the medulla to the hemispheres by the structure's vertical channels. Further, OF's large, straight, and interconnected channels also facilitated the formation of vessels as shown by the central vasculature in horizontal canals (i.e., perpendicular to the slide). In contrast, the haphazard arrangement of the BO and CO particles was unable to drive the bone more than 1–2 mm away from the calvarium.

After 4 months, there was no statistical difference between the materials. The new bone occupied about 40% of the volume under the titanium hemispheres, regardless of the bone substitute. This figure is in agreement with that found with BO in minipigs (Busenlechner et al. 2008). The differences in terms of new bone volume failed to reach statistical significance primarily due to the variance of the data (Fig. 5a). Still, a pattern emerged showing somewhat more bone formed in CO sites. One explanation relates to the degradation rate of CO as compared to the two others substitutes. Indeed, OF and BO demonstrated only little evidence of material degradation either at 2 or 4 months. By comparison, the volume of bone substitutes decreased by 1.7 times in CO samples. It follows that the material's resorption left space for the new bone to fill. This increase in degradation rate (relative to OF and BO) is probably due to a difference in chemical composition. CO is made of pure β-TCP, while OF is made of α-TCP and microcrystalline, calcium-deficient hydroxyapatite. α-TCP, which is more soluble than β-TCP, converts to HA in contact with body fluids and is known for its low rate of degradation (Lin et al. 2001; Munar et al. 2006). Still, the persistence of OF past the initial 4 months may increase the mechanical resistance of the new tissue when compared to other bone substitutes, insofar as about 90% of the available volume is filled either with bone or with substitute material. Also, in OF samples, a slight evolution into adipocytic bone marrow was occasionally observed in isolated bone lacunae—a finding which indicates a high degree of bone maturity and vitality. Still, further studies are needed to confirm these findings, and longer studies will clarify the kinetics of OF resorption.

BO and CO are generally implanted as particles which are enclosed in a resorbable membrane that ensures stability and prevents leakage of the particles into the surrounding

soft tissue. This technique has become a standard of treatment but cannot be easily applied to substantially increase the height of the jawbones. In contrast, OF is manufactured as a block which can be readily shaped to conform to the underlying bone's morphology and is then screw-fastened. This results in a high mechanical stability that also provides support for the overlying gingiva. The logical evolution of the product is the fabrication of individually tailored constructs made to conform to a patient's needs as derived from 3D imaging procedures.

Conclusion

When compared to existing bone substitutes, the 3D block OsteoFlux® enhances vertical bone growth during the first 2 months after implantation in a sheep calvarial model. The blocks function as a scaffold with a regular arrangement of interconnected pores. They provide an osteoconductivity that results in an amount of bone 3 mm away from the bony bed that is 4 times greater than that obtained with the two other substitutes during the first two months. These are promising results which must be confirmed in clinical tests.

Acknowledgements: The authors are indebted to NAMSA-Lyon, France. Particular thanks go to Dr. S. Chirat, Dr. A. Letessier, and Dr. A. Alves. We are also grateful to Karr Dental AG (Thalwil, CH) for providing the Bio-Oss® material.

References

Busenlechner, D., Tangl, S., Mair, B., Fugger, G., Gruber, R., Redl, H. & Watzek, G. (2008) Simultaneous *in vivo* comparison of bone substitutes in a guided bone regeneration model. *Biomaterials* **29**: 3195–3200.

Daculsi, G. (1998) Biphasic calcium phosphate concept applied to artificial bone, implant coating and injectable bone substitute. *Biomaterials* **19**: 1473–1478.

Draenert, F.G., Huetzen, D., Neff, A. & Mueller, W.E. (2014) Vertical bone augmentation procedures: basics and techniques in dental implantology. *Journal of Biomedical Materials Research Part A* **102**: 1605–1613.

Esposito, M., Grusovin, M.G., Felice, P., Karatzopoulos, G., Worthington, H.V. & Coulthard, P. (2009) Interventions for replacing missing teeth: horizontal and vertical bone augmentation techniques for dental implant treatment. *Cochrane Database Systematic Reviews* **7**: CD003607.

Eufinger, H., Rasche, C., Lehmbrock, J., Wehmoller, M., Weihe, S., Schmitz, I., Schiller, C. & Epple, M. (2007) Performance of functionally graded implants of polylactides and calcium phosphate/calcium carbonate in an ovine model for computer assisted craniectomy and cranioplasty. *Biomaterials* **28**: 475–485.

Felice, P., Marchetti, C., Iezzi, G., Piattelli, A., Worthington, H., Pellegrino, G. & Esposito, M. (2009) Vertical ridge augmentation of the atrophic posterior mandible with interpositional bloc grafts: bone from the iliac crest vs. Bovine anorganic bone. Clinical and histological results up to one year after loading from a randomized-controlled clinical trial. *Clinical Oral Implants Research* **20**: 1386–1393.

Gosain, A.K., Riordan, P.A., Song, L., Amarante, M.T., Kalantarian, B., Nagy, P.G., Wilson, C.R., Toth, J.M. & McIntyre, B.L. (2004) A 1-year study of osteoinduction in hydroxyapatite-derived biomaterials in an adult sheep model: part ii. Bioengineering implants to optimize bone replacement in reconstruction of cranial defects. *Plastic and Reconstructive Surgery* **114**: 1155–1163; discussion 1164–1155.

Gross, J.S. (1997) Bone grafting materials for dental applications: a practical guide. *Compendium of Continuing Education in Dentistry* **18**: 1013–1018, 1020–1012, 1024, passim; quiz.

Hollister, S.J., Lin, C.Y., Saito, E., Schek, R.D., Taboas, J.M., Williams, J.M., Partee, B., Flanagan, C.L., Diggs, A., Wilke, E.N., Van Lenthe, G.H., Muller, R., Wirtz, T., Das, S., Feinberg, S.E. & Krebsbach, P.H. (2005) Engineering craniofacial scaffolds. *Orthodontics and Craniofacial Research* **8**: 162–173.

Karageorgiou, V. & Kaplan, D. (2005) Porosity of 3d biomaterial scaffolds and osteogenesis. *Biomaterials* **26**: 5474–5491.

Kuemmerle, J.M., Oberle, A., Oechslin, C., Bohner, M., Frei, C., Boecken, I. & von Rechenberg, B. (2005) Assessment of the suitability of a new brushite calcium phosphate cement for cranioplasty - an experimental study in sheep. *Journal of Cranio-Maxillofacial Surgery* **33**: 37–44.

Lin, J.H., Kuo, K.H., Ding, S.J. & Ju, C.P. (2001) Surface reaction of stoichiometric and calcium-deficient hydroxyapatite in simulated body fluid. *Journal of Materials Science: Materials in Medicine* **12**: 731–741.

Munar, M.L., Udoh, K., Ishikawa, K., Matsuya, S. & Nakagawa, M. (2006) Effects of sintering temperature over 1300 degrees c on the physical and compositional properties of porous hydroxyapatite foam. *Dental Materials Journal* **25**: 51–58.

Myeroff, C. & Archdeacon, M. (2011) Autogenous bone graft: donor sites and techniques. *Journal of Bone and Joint Surgery American* **93**: 2227–2236.

Pearce, A.I., Richards, R.G., Milz, S., Schneider, E. & Pearce, S.G. (2007) Animal models for implant biomaterial research in bone: a review. *Journal of European Cells and Materials* **13**: 1–10.

Polo-Corrales, L., Latorre-Esteves, M. & Ramirez-Vick, J.E. (2014) Scaffold design for bone regeneration. *Journal of Nanoscience and Nanotechnology* **14**: 15–56.

Richardson, C.R., Mellonig, J.T., Brunsvold, M.A., McDonnell, H.T. & Cochran, D.L. (1999) Clinical evaluation of bio-oss: a bovine-derived xenograft for the treatment of periodontal osseous defects in humans. *Journal of Clinical Periodontology* **26**: 421–428.

Seitz, H., Rieder, W., Irsen, S., Leukers, B. & Tille, C. (2005) Three-dimensional printing of porous ceramic scaffolds for bone tissue engineering. *Journal of Biomedical Materials Research Part B: Applied Biomaterials* **74**: 782–788.

Simion, M., Rocchietta, I., Kim, D., Nevins, M. & Fiorellini, J. (2006) Vertical ridge augmentation by means of deproteinized bovine bone block and recombinant human platelet-derived growth factor-bb: a histologic study in a dog model. *International Journal of Periodontics and Restorative Dentistry* **26**: 415–423.

Wenz, B., Oesch, B. & Horst, M. (2001) Analysis of the risk of transmitting bovine spongiform encephalopathy through bone grafts derived from bovine bone. *Biomaterials* **22**: 1599–1606.

Yamada, Y., Nanba, K. & Ito, K. (2003) Effects of occlusiveness of a titanium cap on bone generation beyond the skeletal envelope in the rabbit calvarium. *Clinical Oral Implants Research* **14**: 455–463.

Yamada, Y., Tamura, T., Hariu, K., Asano, Y., Sato, S. & Ito, K. (2008) Angiogenesis in newly augmented bone observed in rabbit calvarium using a titanium cap. *Clinical Oral Implants Research* **19**: 1003–1009.